**Journal of Ultrafine Grained and Nanostructured Materials**
https://jufgnsm.ut.ac.ir
Vol. 53, No.1, June 2020, pp. 48-59
Print ISSN: 2423-6845 Online ISSN: 2423-6837
DOI: 10.22059/jufgnsm.2020.01.07

# Experimental and Numerical Investigation of Mechanical Properties in the Ultrasonic Assisted constraint groove pressing process of copper sheets

***M Asgari, M Honarpisheh*, H Mansouri***

*Faculty of Mechanical Engineering, University of Kashan, Kashan, Iran.*

*Recieved: 20 March 2020; Accepted: 8 June 2020*
** Corresponding author email: honarpishe@kashanu.ac.ir*

**ABSTRACT**

In this study, constraint groove pressing (CGP) process and ultrasonic assisted CGP (UCGP) process were investigated on the process forces, mechanical properties of the sheet, including hardness and tensile tests and grain size. Pure copper sheets were used as samples in this research. Samples were tested both with and without ultrasonic vibrations for mechanical properties and grain size up to 4 passes. The results of tensile tests showed that by applying CGP process, the strength of the samples increases significantly in the first two passes and then decreases. Hardness test results showed an increase which had the highest rate after the first pass. As expected, CGP process was very effective to create fine-grained metal structure. Also, process forces were investigated in both CGP and UCGP processes and then compared in 3 methods of 2 dimension (plane strain) simulation, 3 dimension simulation and experimental examination. After all, a good agreement was achieved.

***Keywords:*** *constraint groove pressing; ultrasonic vibrations; finite element; mechanical properties.*

## 1. Introduction

Grain size refinement is an important method of strengthening the materials compared to other strengthening methods. By using severe plastic deformation (SPD) methods, a good combination of strength and ductility can simultaneously be achieved. While in other methods, strength increase is along with ductility decrease. In addition, it is easier to control mechanical properties in this method. Severe plastic deformations reduce the grain size to nanometer scale by applying strain to the sample, and as a result, significantly, improving the mechanical properties of the metal. The relationship between ultrasonic vibrations and SPD processes can be considered as an important research topic. There are several SPD processes, such as equal channel angular pressing (ECAP) [1], accumulative roll bonding (ARB) [2], high pressure torsion (HPT) [3], equal channel angular rolling (ECAR) [4-7], and simple shear extrusion (SSE) [8, 9]. CGP is one of the most common methods of the SPD processes. In this method, plane strain and pure shear apply while the sample is constrained for dimensional changes and bending strains [10].

The CGP method was introduced in 2002, by Shin et al. (Figure 1). The base of the process is that the metal sheet is pressed in a mold with asymmetrical grooves (Fig. 1-1). The inclined zones of plate are deformed under shear stresses with a plate-strain situation, and no strain applies to the flat part of the sheet (Unhatched area). With inclination degree of 45° to the grooves, the applied shear strain will be equal to one, and an effective strain of about 0.58 will apply to the sample. In

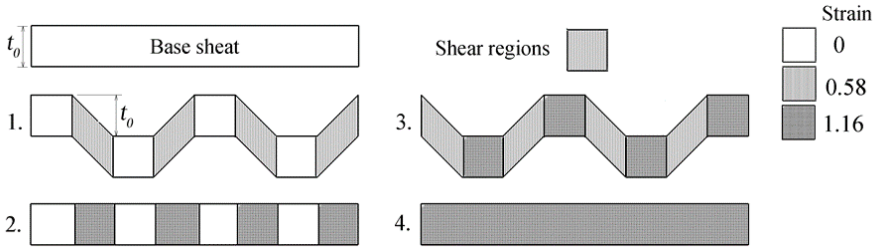


Fig. 1- Schematic illustration of the CGP process principles.

the next step, the sheet is pressed between two flat plates and returns to its original shape, resulting in being re-sheared and doubling their strain in these regions (Fig. 1-2). Then, the sheet metal rotates 180 degrees around the axis normal to the sheet surface and as in the previous steps the shear strain applies to both grooving and straightening states and the strain rate becomes uniform throughout the whole sheet. Repeating these steps results in high strain application on the sheet and converts its texture to an ultra-fine structure [10-12].

In the CGP process, friction should be controlled to avoid as much surface crack creation as possible, which will change into the failure factor in high passes. Kazeminejad et al. investigated the effect of friction reduction by using Teflon layers as a lubricant. They were able to perform 7 passes of CGP process on pure aluminum samples [13, 14], which in previous studies had a maximum of 4 passes [15, 16].

In last decades, the effects of SPD processes, including ECAE, on the microstructure of steel alloys have been seriously studied, but there are very few reports on the effect of the CGP process on the microstructure and the mechanical properties of these alloys [13]. In a study by Mason et al. the final grain size after 4 passes of CGP reported about 213 nm [17]. The grain fining occurs more in the initial stages of the process up to strains of 2 to 3, and does not apparently change for the higher values of the strain. Instead of grain fining in the dominant microstructural changes for strain values of above 3, the fraction of large-angle boundaries increases [10, 15, 18- 20]. Other studies have reported that with increasing the strain, the distance between these boundaries become smaller and the angle of their dislocations increases [21, 22]. In this regard, various studies have shown that ultra-fine grained materials produced by SPD methods (including the CGP process) have a much better superplastic property than conventional materials produced by conventional methods, even at low temperatures and high strain rates [23, 24]. Hardness and uniformity of the strain were studied for CGPed low carbon steel sheet by Khodabakhshi et al. and it was observed that, unlike the strength that decreases in the high strains, hardness increased with increasing pass numbers [14]. Kumar and Raghu also investigated the hardness of the CGPed nickel sheet, and observed severe hardness increase after the first pass and slight increase in subsequent passes [25]. In another study, Kumar et al. performed hardness measurement of CGPed titanium. Hardness Increase in the first pass was significant and in the second pass was very small [26]. A similar result observed for low-carbon steel [15]. In 2018 Nazari et al. found Von-Mises more suitable yield criterion than Tresca in analytical model of CGP for forces estimation [27], and in another research in the same year they investigated deformation behavior on the CGPed sheet [28]. In 2019 they also investigated residual stress of copper sheet in the CGP process and reported a decrease in residual stresses by increasing number of process passes [29]. Severe plastic deformation methods reduce the grain size to nanoscale size and improve the mechanical properties of the metal. Also, they have recently investigated the effect of microstructure parameters on the residual stress in the CGP process of copper samples [30].

According to author information there is not much information about the effect of the ultrasonic vibration on the mechanical properties of CGPed sheet. So, experimental and numerical investigation of mechanical properties in the ultrasonic assisted constraint groove pressing process of copper sheets was performed in this study.

## 2. Research Method

### 2.1. Tool Design

In order to run the CGP process, samples should be placed under the press in their own format, but in addition, the ultrasonic components assembly must also be attached to the workpiece. On the other

hand, since the mold has to be vibrating, the design of the mold is different in this process. In rectangular molds, the corners of the workpiece bend, so in this research, the molds are rounded. Flat and grooved molds are called horn here. Concentrator or horn carries the ultrasonic vibrations from transducer to the target area. Its main function is to transmit and amplify the vibration amplitude in order to improve the performance of the ultrasonic system. The horn should have two good mechanical and acoustic features. Thereby, in this research CK45 steel alloy was used with frequency of 20 kHz.

To prepare a vibrating system, it is necessary to clamp the system at certain points to be stable. Because the system is vibrating, these points must be carefully selected so that there is no movement in these points and heat generation is prevented. The resonant frequency obtained from the software for the groove and flat molding was 18616 and 18799 Hz, respectively. The experimental value obtained from the generator for the groove and flat molding was 18.68 and 18.8 kHz, respectively. The results indicate acceptable accuracy of the performed simulation. To perform this test a SIGMASSONIC 2000 W generator with a working frequency of 20 kHz was selected.

In order to create the upper and lower molds, the material was first prepared with a specified diameter and then machined to fit on the workpiece. At this stage, the length of the workpiece was considered to be longer than the length of the vibration tool. Then the designed groove and extra length of the workpiece was machined by EDM operation. The extra part was used for the bottom mold. A similar part was also made for flat mold. The bottom molds were set in the fixture which is shown in Figure 2.

A screw was designed on the fixture to prevent rotation of the bottom mold. For the sake of simplicity, the bottom fixture was considered in square shape, and then the lower jaws of the mold were placed inside it. In order to remove the sheets after the process easily, a hole was embedded underneath the bottom mold place on the fixture. A tube fixture was designed to keep the transducer inside and connect the mold to the assembly, and then the fixture attached to the press machine. This fixture also considered as a protective device for the transducer to prevent possible blows (Fig. 3a). Figure 3b shows the image of the used transducer in this study.

In the application of ultrasonic waves, wavelengths can be calculated by the relations (1) to (4), using two variables of frequency and velocity.

$$C = \sqrt{\frac{E}{\rho}} = \sqrt{\frac{210000}{7.8 \times 10^{-3}}} \frac{MPa}{(g/mm^3)} \approx 5200\ (m/s) \quad (1)$$

$$\lambda = \frac{C}{f} = \frac{5200}{20000} \frac{(m/s)}{s^{-1}} = 0.26\ m = 260\ mm \quad (2)$$

The largest diameter of the vibrating instrument must be less or equal to one-fourth of the longitudinal vibrational wavelength for the desired frequency. So:

$$D_{max} = \frac{\lambda}{4} = \frac{260}{4} = 65\ mm \quad (3)$$

If this condition is not satisfied, the effect of transverse vibrations in the concentrator will be considerable and it'll lead to waste of energy. The length of the horn is calculated from equation (4):

$$L = n\ \frac{\lambda}{2} \overset{n=1}{\Longrightarrow} L = 130\ (mm) \quad (4)$$

Fig. 2- Fixture and bottom part of flat and grooved molds.

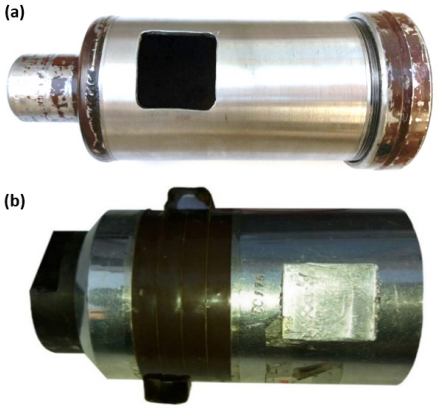


Fig. 3- (a) designed fixture for mold and transducer (Transducer Protector), (b) used transducer.

In the formulas above, $D_{max}$ is the largest diameter of the vibrating instrument, λ is the longitudinal wavelength of the vibration, L is the length of the horn, C is the longitudinal wavelength (compressive), E is the young's module, ρ is density and f is the frequency.

The dimensions of the groove in the grooved mold depend on the design of the mold and the thickness of the sheet. Therefore, molds are designed and made for sheets of 3 mm thick.

### 2.2. Mechanical Properties

After the CGP process, tensile test samples were prepared from deformed samples. The test sample length was selected in perpendicular direction to the grooves. The dimensions are shown in Figure 4, according to ASTM-STP1576 standard. All tests were performed at ambient temperature, using HOUNSFIELD tensile test device. Figure 5 indicates the prepared sample for the tensile test.

In order to evaluate the hardness variations in the specimens and the homogeneity of deformation, a Vickers hardness test was performed. This test was done in two ways:

1- On the surface of the sheet perpendicular to the grooves.

2- Through the thickness of the sheet.

The hardness was obtained from the average of at least 3 hardness measurements along these lines in different situations.

In order to evaluate the effect of CGP process on the grain size, images of the CGPed copper microstructure was prepared by optical microscopy. First, the pieces were arranged together, and after grinding with 80, 120, 400, 800, 1200 and 2000 rubs, the specimens were finally polished with mixed of water and $Al_2O_3$. A solution with 100 ml of alcohol and 100 ml of HCl and about 5 gr of copper chloride ($CuCl_2$) was used to manifest the grains. Images were captured from the sample structure by optical microscope.

### 2.3. Finite Element Modeling

A finite element simulation in ABAQUS software was used to analyze the concentrator. It is possible to obtain the longitudinal, torsional and bending resonance frequencies of the piece by modal analysis. To increase and decrease the length, and to create grooves, easily, the flange location must be positioned exactly on the node. The part design was done by CATIA software first, and then files stored in STEP format and loaded in ABAQUS software. For the analysis of grooved and flat molds, the deformable part with C3D10 type mesh was used with the number of elements of 70570 and 69277, respectively. The meshes were as small as possible. Clearly, any finer element meshing results in higher mesh accuracy, but on the other hand, the equation solving time in the ABAQUS software is increased so that we can reduce mesh size to a certain extent. The mesh size was measured in 5 different sizes to achieve convergence of results. After the analysis of the molding, the length of the resonant frequency was 18616 Hz for the grooved mold and 18799 Hz for the flat mold. Figure 6 shows the tooling system for the finite element analysis.

When simulation results are comparable to practical experiments numerical simulation can provide technical support for designers. This simulation was performed using the Dynamic/ Explicit method of CGP process FEM modeling in ABAQUS software. Adaptive mesh techniques were used to improve shapes of the elements. In the simulation of each pressure step, the lower die was fully fixed in all directions and angles, and the upper die was lowered by only 3 mm in the vertical direction. In this study, the Johnson-Cook model was used to simulate the CGP process. This model is a visco-plastic material model based on strain and temperature that describes the relationship between stress, strain, strain rate and temperature. This is appropriate for problems in which the

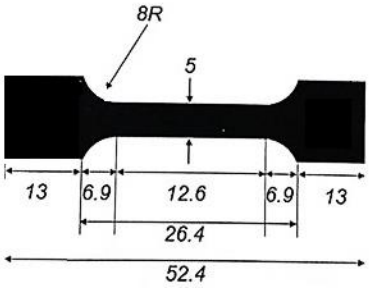


Fig. 4- Dimensions of the tensile test sample according to ASTM-STP1576 standard.

Fig. 5- Prepared Sample for Tensile Test.

strain rate varies at a high range and the generated temperature by the plastic deformation changes by thermal softening. In this model, the effective yield stress is obtained according to equation (5) [31].

$$\bar{\sigma} = [A + B\bar{\varepsilon}^{n}] \times \left[1 + C\, ln\left(\frac{\dot{\varepsilon}}{\dot{\varepsilon}_0}\right)\right] \times \left[1 - \left(\frac{T - T_0}{T_m - T_0}\right)^{m}\right] \quad (5)$$

Where $\bar{\sigma}$ is the effective stress, $\bar{\varepsilon}$ is the effective strain, $T_0$ is the ambient temperature and $T_m$ is the melting temperature of the material.

The constant coefficients of this relation are also obtained from the Johnson-Cook coefficient for copper sheets [31], where A is the initial yield stress, B is the hardening module, n is the work-hardening power, C is the coefficient of the strain rate, and m is thermal softening. The used friction coefficient was equal to 0.25 [14].

## 3. Results and discussions

### 3.1. Mechanical Properties

Figure 7 shows tensile behavior of the annealed pure copper in different passes of CGP and UCGP process.

Applying severe strain to the metal will increase the dislocation density which will lead to enhancement of the strength. On the other hand, the increase in strength is equivalent to decrease in the flexibility of the metal, in other words, decreasing the percentage of relative length variation, gives a precise examination of the tensile

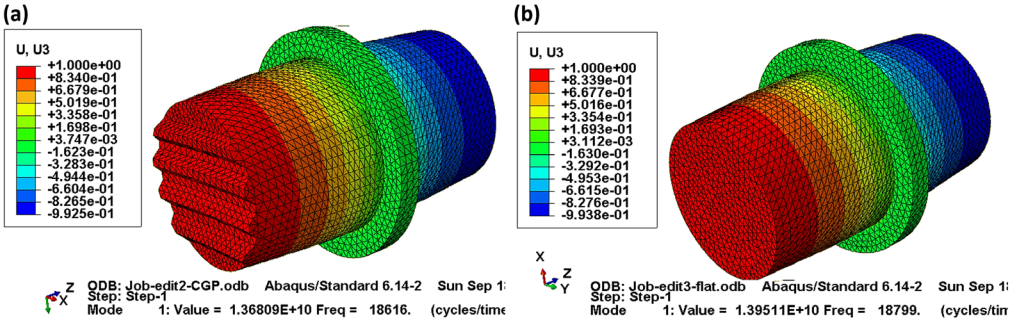


Fig. 6- The first ABAQUS designed longitudinal mode for (a) grooved horn, (b) flat horn.

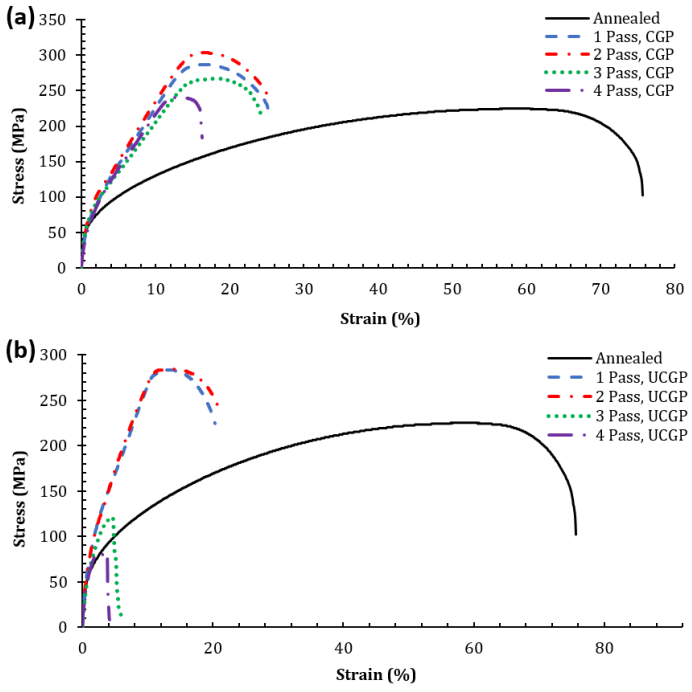


Fig. 7- Effective stress-strain diagram of (a) CGPed samples, (b) UCGPed samples.

behavior of this subject [16].

The results of the tensile test of pure copper samples are obtained in both ultrasonic and non-ultrasonic states. In Figure 8, the results are shown in terms of the number of passes in the CGP and UCGP processes.

As can be seen, the highest rate of UTS and YS occurs in the first pass of the process. The UTS of the samples increased from 224 MPa to 287 MPa for the CGPed samples and 283 MPa for the UCGPed samples. In the second pass, the UTS increase was lower than the first pass. The UTS in the second pass was 303 MPa for the CGPed and 284 MPa for the UCGPed samples. The amount of UTS in subsequent passes decreased, so that in the third and fourth passes, the values of 267 and 240 MPa in UCGP mode and 120 and 83 MPa in CGP mode were obtained. On the other hand, YS of the annealed samples was 60 MPa, which increased to 201 and 164 MPa in the first and second passes, for CGPed samples and 153 and 169 MPa for UCGPed samples, respectively. The YS amount decreased in subsequent passes, and this decrease was greater in UCGP process. The increase of UTS and the YS of copper samples in the first and second passes can be attributed to the work-hardening and the grain fining mechanisms. UTS and YS increases with increasing number of pressing passes, which may be due to the following reasons:

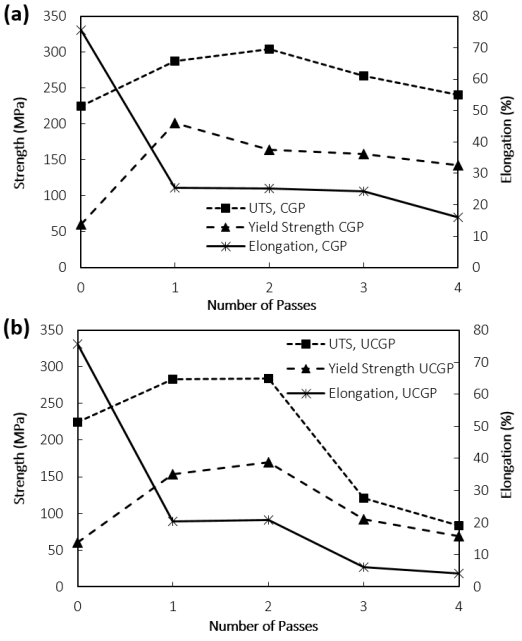


Fig. 8- Results of the tensile test in terms of the number of passes in the (a) CGP, (b) UCGP.

The first is that, as a result of cold working on samples, dislocations are generated and as the amount of applied strain increases, the density of these dislocations increases and they confluence more with each other. Therefore, by increasing the number of pressing passes, the amount of cold work done on the sample is increased, which leads to an increase in the strength of the samples (work hardening). Another reason is that, the application of severe strain generates dislocation boundaries and divides primary grains into smaller units called cell blocks. By increasing the applied strain, the distance between these boundaries becomes smaller and as a result, a microstructure with very fine graining is formed, and thus, the strength increases (grain fining mechanism). Elongation percentage of the samples also decreased in second and third passes comparing to the first pass. The reason of these changes can be attributed to the work hardening [21, 22]. But the reasons for reducing the strength of samples in the third and fourth passes can be explained by two following factors:

First, at the beginning, when the internal energy of the material is low, the speed of processes such as ascending and cross-slipping, which reduces the density of dislocations, is low. Thus, activities that generate dislocation mechanisms are caused rapid growth of dislocations density. Then with the rising energy level of the material, the speed of ascending and cross-slipping increases, and on the other hand, the driving force for processes that use dislocations, increases. Therefore, continuing the deformation decreases the speed of generation of dislocations density and reaches the saturation level. The fall in the density of dislocations in larger strains is also the result of the high amount of dislocation consumption, which represents the fourth pass (dynamic retrieval) [14, 15]. The second reason which recently mentioned in Kazeminejad's research is that the small cracks on the surface of the sample reduce the strength in higher strains [13]. Tensile test was performed to prove the effect of this matter, once, without reducing the thickness and again by reducing the thickness. Reducing UTS and YS of The UCGPed compared to CGPed copper samples can be considered due to the formation of deeper cracks in the samples. Because, mounting vibrating stresses during ultrasonic assisted deformation processes, decreases the static YS [32]. This stress reduction was observed both

in tensile and compressive loading. This factor can be expressed as the main cause of creating deeper cracks in UCGPed samples. Figures 9a and 9b show the throughout hardness diagram of the samples. As we can see, the use of ultrasonic vibrations increases the uniformity of the sample hardness. In Figure 9c, the variations of sample hardness are shown in terms of the number of passes of the CGP and UCGP processes. As can be seen, the hardness of the annealed sample is 52 Vickers, which increased significantly in the first pass of the CGP process and reached 100 Vickers; this increase was lower in subsequent passes. So, the hardness was 111, 116 and 118 Vickers in the second, third, and fourth pass, respectively. Here, the reasons for increasing strength can also verify increasing the hardness in the higher passes, too.

Also, the ultrasonic vibrations usage in the process slightly increased the hardness on the surface of the sheet. The hardness of the specimen after the first pass was 106 Vickers and was 110, 119, and 122 Vickers in the second, third, and fourth passes, respectively. As can be seen, an increase of about 5% of hardness amount is obtained while using ultrasonic vibrations, which is likely due to more work-hardening with presence of ultrasonic vibrations.

Figure 10 also shows the distribution of hardness along the sheet thickness in the CGP and UCGP processes.

In general, the hardness increases by increasing the number of passes, and this increase in the first pass is significant [33]. Hardness improvement is due to an increase in the density of dislocations and

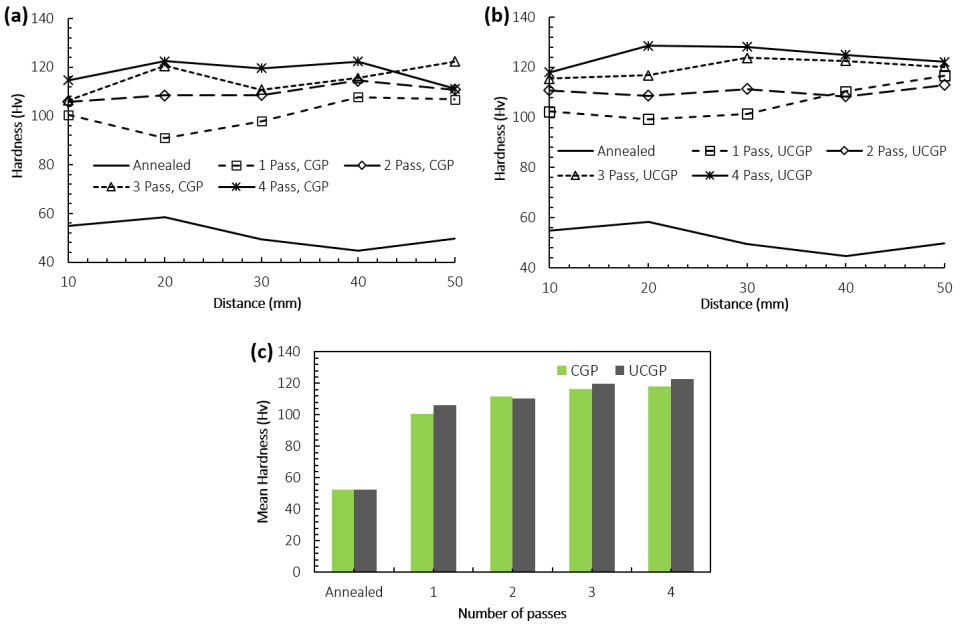


Fig. 9- Hardness distribution along the sheet for (a) CGPed samples, (b) UCGPed samples, (c) Hardness variation at the sample surface in terms of number of passes.

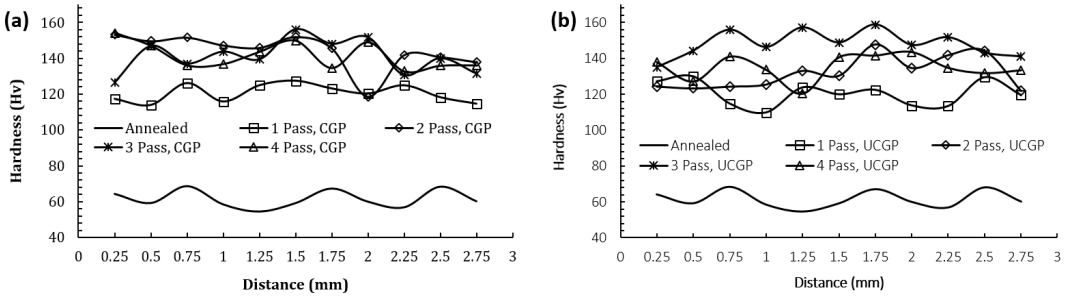


Fig. 10- Hardness distribution along the thickness in the (a) CGP, (b) UCGP process.

work-hardening of materials. Similar results have been reported for the hardness change in other studies of CGPed aluminum [34-36].

### 3.2. Microstructure Evaluation

The most important impact of the CGP process, and, in general, SPD processes, is the reduction in grain size. The microstructure obtained from the optical microscope of annealed and CGPed copper sheets are shown in Figure 11 in various passes.

As can be seen from Fig. 11a, the initial sheet has a microstructure with a grain size of approximately 60 μm. According to the figure, after 4 passes, the grain size has dropped to 12 μm. The grain size has been calculated according to the ASTM standard. Therefore, the CGP process causes severe deformation to the specimens and results in microstructure changes and improvements in mechanical properties. As can be seen in Fig. 11, the left samples with ultrasonic vibrations, have finer grains rather than the right samples. It means that the ultrasonic vibrations make the samples' plastic deformation more severe and assist in improving grain refinement efficiency. After transmission the ultrasonic wave in the copper samples, it can disturb the particles of a body from equilibrium, which gives rise to internal forces that tend to return these particles to equilibrium [37]. The stresses associated with the propagation of ultrasonic wave are the basic cause of the numerous mechanical effects attributable for improving the material microstructure [38].

### 3.3. Process Modeling

During the CGP process, sheets severely deform and large amount of strain applies to them. According to the theory of CGP, the created strain should be homogeneous all over the sample sheet. However, the strain heterogeneity has been observed in practical situations. Figure 12(a) shows the distribution of effective plastic strain at different times during the first pressing. This figure shows that the sheet bends on its surface before shear deformation, so the applied plastic strain to the sample is not a pure shear. Shear deformation mainly occurs on the inclined part of the sheet and bending mainly occurs on the surface of the workpiece. This issue can be considered as one of the reasons for the un-uniformity of the strain. Figure 12b shows the evolution of the strain distribution over a complete cycle of the CGP process and the lack of uniformity at the end of the cycle. Several studies on deformation behavior in CGP copper sheets, using finite element analysis [39], show that there is some inhomogeneity in the sheets, and the average of created strain in the sheet at different stages is more than theoretical value. Figure 12c shows the effective strain values along the CGPed sheet at 4 first pass presses. For the reason of this difference it can be explained that, in the evaluation of the strain theory, the deformation state is assumed as a simple shear, while the deformation during the CGP also involves some tensile and compressive strains. In addition, in theory analysis, it is assumed that there are some areas that remain unchanged and in that theory, the cohesion of the sheet material is not considered [15]. Also, in Figure 12d, effective strain on the surface and middle thickness along the sheet is observed. The amount of strain in the middle of the sheet thickness is more than the created pressure on the surface of the sheet, which is due to the effect of friction. The deformation of the sheet surface is constrained by friction between the mold and the sheet [39].

As a result of performing a CGP process pass, a distribution of the strain occurs on the sheet, and different regions contain less or more strain values. By increasing the number of process passes, the material gets closer to its saturation state, so areas where experienced less strain at previous passes, get a higher strain rate at this pas because of their vacant capacity for becoming saturated. This results of strain balancing in different regions, which leads to uniformity of strain distribution in the sheet at higher passes, and consequently, increasing the number of passes, leads to more uniform distribution of hardness [40].

The shear stress component is greater in inclined regions but it's much less in areas close to the edge of the grooves. Therefore, these areas in the middle of the sheet thickness are deformed by bending before the completion of performance, so the entered plastic strain on the sample is not pure shear strain type. In the next step, the diagrams of three-dimensional simulation forces were compared with the two-dimensional plane strain simulation forces diagrams and experimental performances.

Figure 13a represents the assessment of the required force for deformation during the first phase of the CGP process, and Figure 13b represents forces in the UCGP process.

Since under the plane strain condition, the material is completely bounded and deformed at a certain surface, and all corners of the mold are

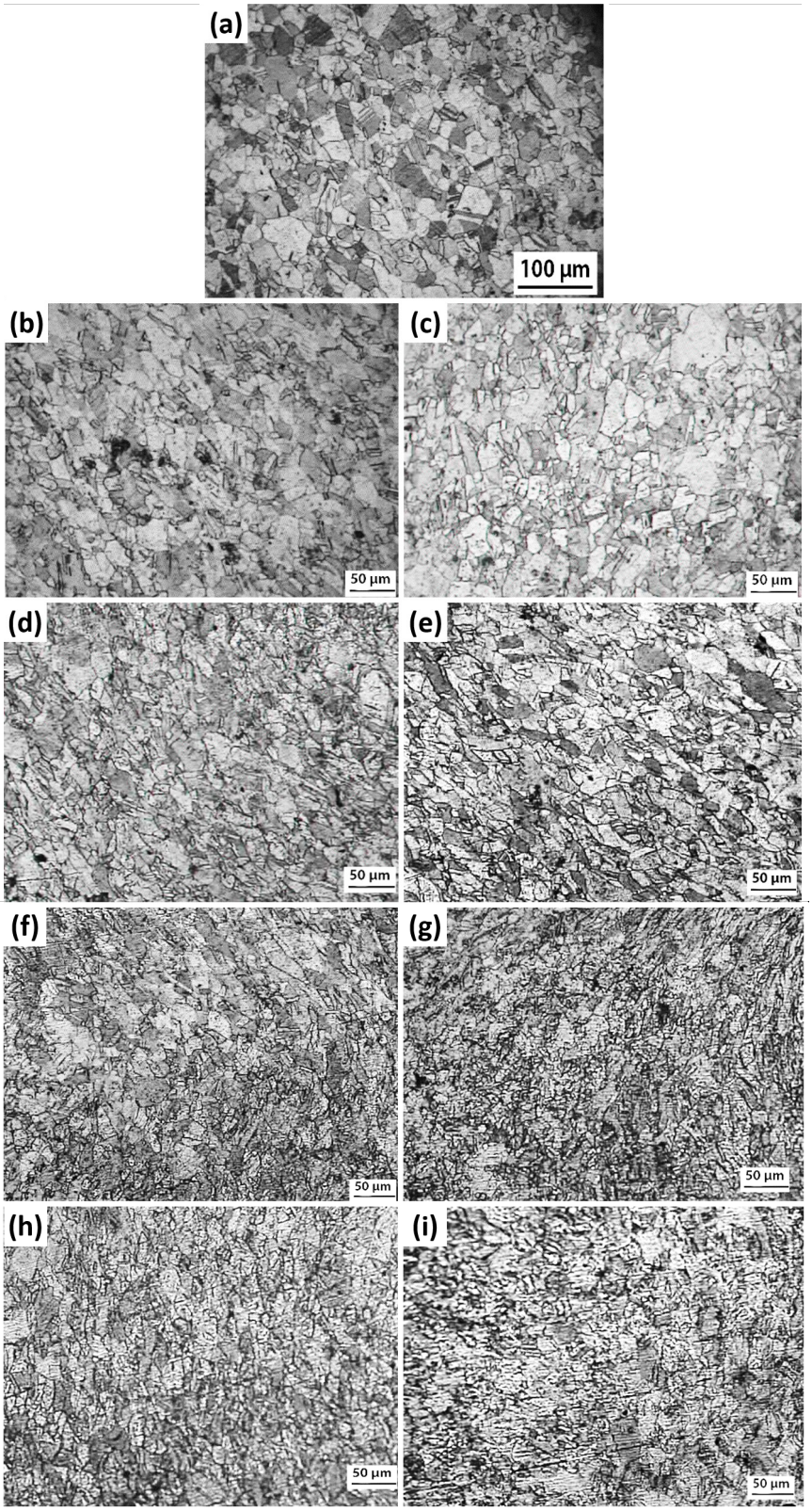


Fig. 11- (a) Optical image taken from the annealed microstructure, optical image taken from the microstructure of the samples after 1 pass of (b) UCGP, (c) CGP, the samples after 2 passes of (d) UCGP, (e) CGP, the samples after 3 passes of (f) UCGP, (g) CGP, the samples after 4 passes of (h) UCGP, (i) CGP.

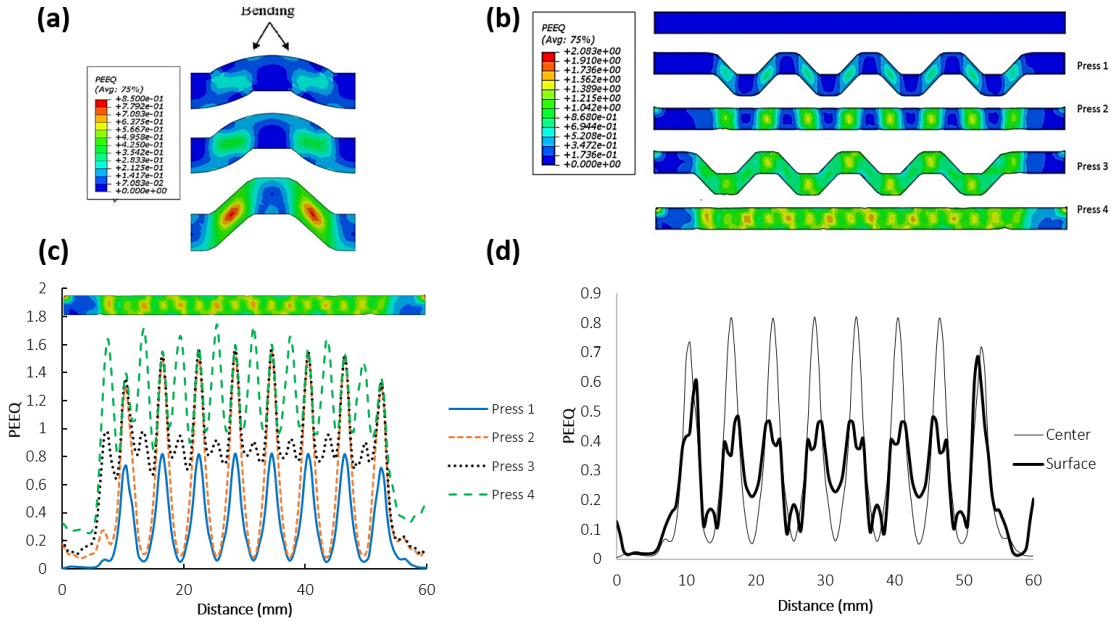


Fig. 12- (a) Distribution of the effective strain at different times for the first pressing (b) Evolution of strain distribution over a complete cycle of the CGP process (c) An effective strain distribution diagram along the CGPed sheet (d) Effective strain distribution at first pressure on the surface and in the middle of the thickness of the CGPed sheet.

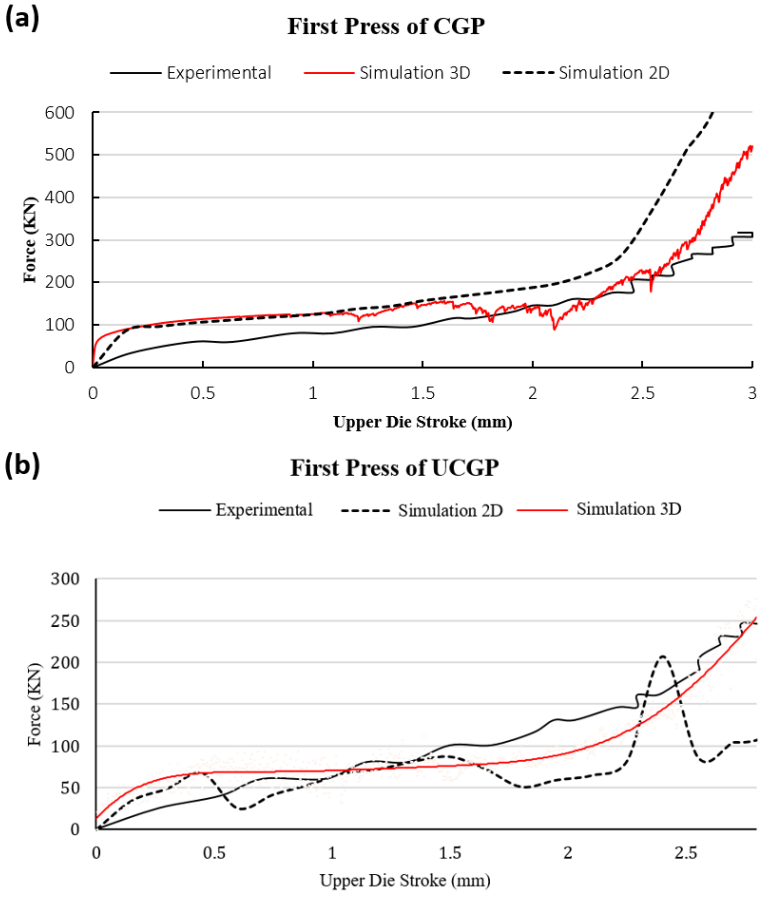


Fig. 13- Force investigation at first pressing of the first pass of (a) CGP process, (b) UCGP process.

Table 1- Process parameters in the CGP and UCP processes

| Process | Pass No. | Yield Strength (MPa) | Tensile Strength (MPa) | Elongation (%) | Process Force (KN) |
|---|---|---|---|---|---|
| CGP | 1 | 201 | 287.3 | 25.4 | 306.6 |
| | 2 | 164.5 | 303.7 | 25.24 | - |
| UCGP | 1 | 153.1 | 283 | 20.32 | 249 |
| | 2 | 169.3 | 284.3 | 20.79 | - |

filled at the end of the upper mold movement, hence, the contact surface between the sample and the particles increases dramatically, which increases the force of deformation. In general, all the simulation results are in a good agreement with the experimental state.

Finally, the Table 1 has been presented to compare the CGP and UCGP processes.

As can be seen from Table 1, the UCGP process does not have a positive effect on the mechanical properties rather than the CGP process.

## 4. Conclusion

In this study, the ultrasonic assisted CGP (UCGP) process was investigated and the effects of process on the mechanical properties and microstructure were studied. Obtained results can be summarized as follows:

- The highest increase in UTS and YS occurs in the first pass of the process. The UTS of the samples increased from 224 MPa to 287 MPa for the CGPed and 283 MPa for the UCGPed specimens.
- The hardness of the annealed specimens was 52 Vickers, which increased to 100 Vickers after the first pass of the CGP process. The hardness increase in the subsequent passes was less.
- The ultrasonic vibrations used in the process slightly increased the hardness on the surface of the sheets. The hardness values after each of 4 passes were 106, 110, 119, and 122 Vickers, respectively. An increase of about 5% of hardness amount is obtained while using ultrasonic vibrations, which is likely due to more work-hardening with presence of ultrasonic vibrations.
- Optical images indicate that the initial sheet has a microstructure with a grain size of approximately 60 μm, which, after 4 passes, reduced to 12 μm.
- By examining the shear stresses in the simulation, it was observed that the shear stress component is higher in inclined regions.
- Force investigation was performed in three ways (2D plane-strain simulation, 3-D simulation and experimental study), and it was observed that the forces in all three examined methods were in a good agreement with each other. Also in the UCGP process a decrease in force was observed after the first pass.

## References


1. Zahari ZS, Awang Sh'ri DN, Abu Hassan MAH, Wan Harun WS. Effect of ECAP die angle to the microstructure and mechanical properties of bulk nanostructured Al-6061. IOP Conference Series: Materials Science and Engineering. 2019;469:012054.
2. Sadeghinia H, Jafarian HR, Salehi MT, Eivani AR. Comprehensive investigation on wear and microstructure development in Al/ti ultrafine grained multi-layered composite produced by Accumulative Roll Bonding (ARB). Materials Research Express. 2019;6(11):116572.
3. Pereira PHR, Huang Y, Langdon TG. Thermal stability and superplastic behaviour of an Al-Mg-Sc alloy processed by ECAP and HPT at different temperatures. IOP Conference Series: Materials Science and Engineering. 2017;194:012013.
4. Honarpisheh M, Haghighat E, Kotobi M. Investigation of residual stress and mechanical properties of equal channel angular rolled St12 strips. Proceedings of the Institution of Mechanical Engineers, Part L: Journal of Materials: Design and Applications. 2016;232(10):841-51.
5. Honarpisheh M, Dehghani M, Haghighat E. Investigation of Mechanical Properties of Al/Cu Strip Produced by Equal Channel Angular Rolling. Procedia Materials Science. 2015;11:1-5.
6. Kotobi M, Honarpisheh M. Uncertainty analysis of residual stresses measured by slitting method in equal-channel angular rolled Al-1060 strips. The Journal of Strain Analysis for Engineering Design. 2016;52(2):83-92.
7. Honarpisheh M, Mansouri H, Saki Entezami S. Investigation of ECAR process on the corrosion behavior of pure commercial copper. Modares Mechanical Engineering. 2017 Dec 10;17(10):39-46.
8. Pardis N, Ebrahimi R. Different processing routes for deformation via simple shear extrusion (SSE). Materials Science and Engineering: A. 2010;527(23):6153-6.
9. Pardis N, Ebrahimi R. Deformation behavior in Simple Shear Extrusion (SSE) as a new severe plastic deformation technique. Materials Science and Engineering: A. 2009;527(1-2):355-60.
10. Shin DH, Park J-J, Kim Y-S, Park K-T. Constrained groove pressing and its application to grain refinement of aluminum. Materials Science and Engineering: A. 2002;328(1-2):98-103.
11. Lee JW, Park JJ. Numerical and experimental investigations of constrained groove pressing and rolling for grain refinement. Journal of Materials Processing Technology. 2002;130-131:208-13.
12. Zehetbauer MJ, Valiev RZ. Nanomaterials by severe plastic deformation. John Wiley & Sons. 2006.
13. Khodabakhshi F, Kazeminezhad M, Kokabi AH. Constrained groove pressing of low carbon steel: Nano-structure and mechanical properties. Materials Science and Engineering: A. 2010;527(16-17):4043-9.

14. Kazeminezhad M, Hosseini E. Optimum groove pressing die design to achieve desirable severely plastic deformed sheets. Materials & Design. 2010;31(1):94-103.
15. Yoon SC, Krishnaiah A, Chakkingal U, Kim HS. Severe plastic deformation and strain localization in groove pressing. Computational Materials Science. 2008;43(4):641-5.
16. Roters F, Raabe D, Gottstein G. Work hardening in heterogeneous alloys—a microstructural approach based on three internal state variables. Acta Materialia. 2000;48(17):4181-9.
17. T. J. Mason, J. P. Lormier, Applied sonochemistry, Weinheim, Germany: Wiley-VCH, 2002.
18. Shirdel A, Khajeh A, Moshksar MM. Experimental and finite element investigation of semi-constrained groove pressing process. Materials & Design. 2010;31(2):946-50.
19. Krishnaiah A, Chakkingal U, Venugopal P. Applicability of the groove pressing technique for grain refinement in commercial purity copper. Materials Science and Engineering: A. 2005;410-411:337-40.
20. Estrin Y, Tóth LS, Molinari A, Bréchet Y. A dislocation-based model for all hardening stages in large strain deformation. Acta Materialia. 1998;46(15):5509-22.
21. Hansen N, Huang X, Hughes DA. Microstructural evolution and hardening parameters. Materials Science and Engineering: A. 2001;317(1-2):3-11.
22. Reihanian M, Ebrahimi R, Tsuji N, Moshksar MM. Analysis of the mechanical properties and deformation behavior of nanostructured commercially pure Al processed by equal channel angular pressing (ECAP). Materials Science and Engineering: A. 2008;473(1-2):189-94.
23. Zhu YT, Lowe TC, Langdon TG. Performance and app lications of nanostructured materials produced by severe plastic deformation. Scripta Materialia. 2004;51(8):825-30.
24. Verlinden B. Severe plastic deformation of metals. Metalurgija-Journal of Metallurgy. 2005;11(3):165-82.
25. Satheesh Kumar SS, Raghu T. Mechanical behaviour and microstructural evolution of constrained groove pressed nickel sheets. Journal of Materials Processing Technology. 2013;213(2):214-20.
26. Kumar GVP, Niranjan GG, Uday C. Grain Refinement in Commercial Purity Titanium Sheets by Constrained Groove Pressing. Materials Science Forum. 2011;683:233-42.
27. Nazari F, Honarpisheh M. Analytical model to estimate force of constrained groove pressing process. Journal of Manufacturing Processes. 2018;32:11-9.
28. Nazari F, Honarpisheh M. Analytical and experimental investigation of deformation in constrained groove pressing process. Proceedings of the Institution of Mechanical Engineers, Part C: Journal of Mechanical Engineering Science. 2018;233(11):3751-9.
29. Nazari F, Honarpisheh M, Zhao H. Effect of stress relief annealing on microstructure, mechanical properties, and residual stress of a copper sheet in the constrained groove pressing process. The International Journal of Advanced Manufacturing Technology. 2019;102(9-12):4361-70.
30. Nazari F, Honarpisheh M, Zhao H. The effect of microstructure parameters on the residual stresses in the ultrafine-grained sheets. Micron. 2020;132:102843.
31. Johnson GR, Cook WH. A constitutive model and data for metals subjected to large strains, high strain rates and high temperatures. InProceedings of the 7th International Symposium on Ballistics 1983 Apr 19 (Vol. 21, No. 1, pp. 541-547).
32. Winsper CE, Sansome DH. A REVIEW OF THE APPLICATION OF OSCILLATORY ENERGY TO METALS DEFORMING PLASTICALLY. Advances in Machine Tool Design and Research 1967: Elsevier; 1968. p. 1349-60.
33. Gupta AK, Maddukuri TS, Singh SK. Constrained groove pressing for sheet metal processing. Progress in Materials Science. 2016;84:403-62.
34. Zrnik J, Kovarik T, Novy Z, Cieslar M. Ultrafine-grained structure development and deformation behavior of aluminium processed by constrained groove pressing. Materials Science and Engineering: A. 2009;503(1-2):126-9.
35. Zrnik J, Vitez I, Kovarik T, Cieslar M. FORMING OF ULTRAFINE GRAINED STRUCTURE IN ALUMINIUM BY CGP METHOD. Metalurgija. 2009 Jan 1;48(1).
36. Zrník J, Kovařík T, Cieslar M. CGP forming method Ti produce ultrafine grained structure in aluminium. Metal. 2008;2008:1-7.
37. Liu Y, Suslov S, Han Q, Hua L, Xu C. Comparison Between Ultrasonic Vibration-Assisted Upsetting and Conventional Upsetting. Metallurgical and Materials Transactions A. 2013;44(7):3232-44.
38. Ensminger D, Stulen FB, editors. Ultrasonics: data, equations and their practical uses. CRC press; 2008 Dec 17.
39. Mori E, Inoue M. Effects of drawing speed and backward tension application of ultrasonic vibration to metal wire drawing (2nd report). J. JSTP. 1970;11:144.
40. Ghazani MS, Vajd A. Finite Element Analysis of the Groove Pressing of Aluminum Alloy. Modeling and Numerical Simulation of Material Science. 2014;04(01):32-6.